

# On the development of a regulating valve design with improved cavitation characteristics

Michael P. Levitsky<sup>1,\*</sup> and Semyon P. Levitsky<sup>2</sup>

<sup>1</sup>*Institute for Industrial Mathematics, Beer-Sheva 84311, Israel*

<sup>2</sup>*Sami Shamoon College of Engineering, Beer-Sheva 84100, Israel,*

*\*Corresponding author: levitsky@iimath.com*

Received 2 April 2006, revised 5 June 2006, accepted 8 June 2006

## Abstract

Under investigation is the basic structure of a valve with a vortex chamber as final-control element, made with tangential ducts so as to create opposing flows. The hydraulic characteristics of the valve are obtained theoretically and experimentally. The reason is substantiated why swirling the flow before the orifice improves its cavitation characteristic. A valve design is proposed, which, besides regulating the flow rate, can function as a shut-off device. The cavitation characteristics of the valve are described at different positions of the regulating element.

**Keywords:** Vortex valve, swirl chamber, cavitation characteristic, control fluid flows, regulating element, pressure drop, pressure source, nozzle.

## 1 Introduction

Regulating and shut-off valves make up a considerable part of the equipment for multiphase flow control in modern industry, power plants, mineral extraction, in pneumohydraulic sections of various mechanisms etc. They can be used for maintaining preset flow rates under constant high resistance, as well as to modify the resistance and flow rates by moving or turning the final-control element of the system according to a given program.

Improvements in production processes, raising of power plants capacities have brought about an increase in the parameters of working media, in particular flow rates, pressures and pressure differences at which the valves operate.

Analysis of the existing problems in hydraulic control equipment for high pressure and flow rate multiphase transport pipelines shows that development of a new valve capable of providing high hydraulic resistance (about 30–40 MPa and even more, if necessary) represents now a vital task.

The operation of hydraulic control equipment under high pressures is characterized by vibration, flow rate pulsations, erosion of the operating units, noise [1]. This reduces the valve's service life and raises the power consumption by the drive.

All such valves are susceptible to severe cavitation. Hydraulic engineers have to accept cavitation in their machines or components. They know that many points of the process are not clearly understood, as for instance the formation of cavities by cavity shedding or interaction between the fluid and the material at the end of collapse. The result of the final collapse is cavitation erosion [2, 3].

Much has been written about cavitation from control valves and how to prevent or control it. To overcome these drawbacks valves using multi-stage throttling have been designed, helping to lower vibration and raising the valve's reliability [4]. Another solution is realized in tortuous path valves that differ in the manner in which pressure drop stages are achieved and in the amount of division in the main flow stream [5].

However, technical solutions of this kind are complex both in design and technology. Besides, such a valve is not effective enough in ensuring the uniform distribution of hydraulic resistance between the stages, which complicates the use of the valve as a shut-off element as well.

Pressure regulating valves of other designs employ a swirl chamber to lower the fluid pressure. Valves that use flow swirling to control the flow rate are known as vortex valves. A vortex valve has an improved cavitation characteristic, is easy to manufacture and capable of fast response, it can operate reliably in a practically unrestricted range of pressure drops and high temperatures. The means to inject the liquid into the vortex chamber and to discharge it towards the final-control elements so as to obtain the required characteristics of the vortex chamber are highly varied, which results in the diversity of vortex valve designs.

Vortex valves normally have at least one radial supply inlet and one or more tangential control inlets [6]. For optimum outlet flow modulation, the radial or supply pressure must be held constant, and the control pressure

must be higher by 1.2 to 2.0 times than the supply pressure at the minimum flow condition. If a single power source is available, an orifice restrictor must be used in series with the supply flow to provide the working pressure differential between the supply and control pressures.

Valves have recently been suggested for flow control under the above conditions with the use of swirling flows, which has a number of advantages. In the present paper the operational parameters are discussed of such a valve and methods for improving its characteristics.

To eliminate the above-listed drawbacks a vortex valve is proposed in which interaction between opposing tangential flows is used [7]. The results of the theoretical and experimental research are presented here, on the basis of which a valve design is proposed using this outline scheme for the vortex chamber. The physical background of the study can be outlined as follows.

Throttling of liquid flow at high pressure drops is usually accompanied by cavitation. It appears in the vicinity of the cross-section corresponding to maximum flow velocity, where the local pressure becomes smaller than saturated vapor pressure at the given temperature. Within the cavitation region vapor-filled bubbles arise, which collapse immediately outside it when the pressure is restored. This process is characterized by formation of high-speed liquid microjets interacting with the internal surface of the operating unit. Numerous studies, both theoretical and experimental [8], have shown that the speed of such microjets is of the order of  $v \sim 100 - 300$  m/s. According to the Corteveg-Joukowski water-hammer theory, the pressure excess in such a jet meeting solid surface can be estimated as  $\Delta p \sim \rho v c \sim 300$  MPa. This estimate explains the microdestruction of the surface material, called cavitation erosion.

Pressure reduction in valves of a typical design results from the stream throttling through a passage with the diameter  $d$  that is much smaller than that of the supply pipeline  $D$ . When the pressure drop is large enough, the abrupt constriction of the flow causes cavitation. The intensity of the latter is characterized by the cavitation number  $K_v = \frac{p_{in} - \tilde{p}_{out}}{p_{in} - p_s}$ , which depends significantly on the  $d/D$  ratio. Here  $p_{in}$  is the inlet pressure,  $\tilde{p}_{out}$  the outlet pressure at the passage corresponding to the onset of cavitation,  $p_s$  the saturated vapor pressure of the liquid at the given temperature. The maximum pressure drop in the valve that can be achieved without cavitation is equal to  $\Delta p_{max} = K_v(p_{in} - p_s)$ . Cavitation usually appears when the ratio  $p_{out}/p_{in} < 0.3 - 0.5$  [9] (the exact value of this ratio depends on a number of reasons: the temperature, liquid properties, form and roughness of the orifice edge, etc.).

The above-described flow pattern is not the only one enabling pressure

to be handled within the valve. An essentially different structure is formed when the pressure is handled in a swirling flow. Swirling permits nuclear cavitation to be transformed into cavitation of another kind – developed cavitation that has important advantages over the former. In a swirling flow, due to the tangential component of velocity, the pressure is redistributed along the radius [10]. As a result, when such a flow passes through a short vortex chamber, the effective cross-section for the axial stream is essentially decreased. Denoting its diameter before the orifice as  $D_{eff}$ , we receive  $d/D_{eff} > d/D$ , where  $D$  is the chamber’s internal diameter. The larger the swirl intensity, the smaller is the value of  $D_{eff}/D$  [11]. For this reason the magnitude of the stream compression is reduced, which raises the cavitation number  $K_v$ . Besides, the action of centrifugal forces prevents the flow separation from the nozzle surface and from the outlet pipeline wall. This depresses the hydrodynamic instability and intensity of vortices in the region adjacent to the orifice.

Another peculiarity of the vortex flow should also be noted. Air bubbles arising in the liquid for diverse reasons are quickly pushed towards the axis of the vortex chamber under the action of the radial pressure gradient. Near the axis the pressure value may be considerably smaller than the pressure of saturated vapor. This leads to additional release of the gas dissolved in the liquid and free gas is collected in the near-axis region where a closed vapor-filled vortex is formed. This property of the vortex flow plays an important role in preventing the impact of the free gas on the total flow stability arising in the inlet channel of the vortex chamber as a result of local cavitation [12].

Thus the vortex chamber ensures effective transformation of nuclear cavitation into developed cavitation, which precludes direct contact of pulsating and collapsing bubbles with the operating surfaces of the valve. As a result, cavitation erosion of the operating unit is also prevented, which prolongs the service life of the device. Therefore high-pressure drop valves using swirling flows are preferable to the usual ones, and the problem of their modeling is therefore of great interest.

## **2 The basic outline of a vortex valve and the main ratios for the computation of its flow rate characteristic**

The basic principle of such a vortex valve, shown in Fig. 1, can be summarized as follows. With equal flow rates through the tangential ducts of the vortex chamber the flow is not swirled and its resistance is minimal. By

shutting off the supply pipeline to one of the ducts the flow swirl is increased as well as the hydraulic resistance to the flow through the valve.

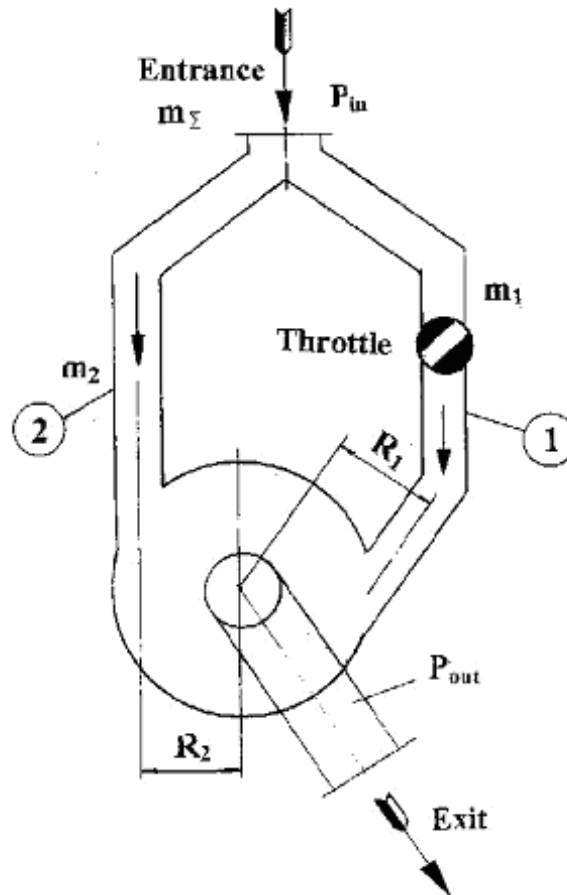


Figure 1: The basic outline of a vortex valve with opposite flows.

Thus the operation of such a vortex valve does not require a controlling flow with a higher pressure level, the distributing element is mounted on the pipeline through which no more than half the working medium flow rate is supplied, and it is loaded with only a small pressure drop, since the main resistance to the outflow is created in the coaxial opening of the vortex chamber – its outlet nozzle. The above-listed distinctions of this scheme simplify the design of the vortex valve, enhance its reliability, eliminate high-

precision friction pairs working under high pressure differentials, and enable the use of much less powerful drives to control the distributing element.

The flow structure within the vortex chamber with intense swirling is characterized as follows. The liquid flow towards the outlet nozzle is mostly structured as running down the end walls of the chamber, with the axial component of the flow velocity appearing at radius  $r_1$ , a little larger than the radius of the nozzle [10, 12]. The flow is realized through an annular cross-section within the nozzle bounded by the radii of the nozzle and the vortex, the latter rotating like a solid body with the pressure on its surface equal to the outlet pressure. Strong reverse flows exist inside the vortex. With the increased distance from the outlet nozzle the flow swirl is damped and the vortex diameter is eventually reduced to zero.

Consider the basic outline of the vortex valve (Fig. 1). The flow entering the chamber through the tangential ducts, positioned at radii  $R_1$  and  $R_2$ , merge into one flow, whose resultant angular momentum equals:

$$m_\Sigma V_{in} R = m_2 V_{in2} R_2 - m_1 V_{in1} R_1. \quad (1)$$

Expressing the values of  $V_{in2} R_2$  and  $V_{in1} R_1$  by the flow rates, bring formula (1) to the following form:

$$V_{in} R = \frac{m_\Sigma}{\rho F_2} R_2 B, \quad B = 1 - 2 \frac{m_1}{m_2} - \left( \frac{m_1}{m_\Sigma} \right)^2 \left( \frac{F_2 R_1}{F_1 R_2} - 1 \right). \quad (2)$$

The liquid flow in the vortex chamber of the valve is described by the equations:

$$ur = V_{in} R, \quad (3)$$

$$p + \Delta p_2 + \frac{\rho}{2} (u^2 + w^2) = p_{in} + \frac{\rho}{2} w_\Sigma^2. \quad (4)$$

As was obtained in [13], the flow in the nozzle passes through an annular cross-section whose area equals

$$F = \pi \left( 1 - \frac{r_m^2}{r_{out}^2} \right) r_{out}^2 = \varphi \pi r_{out}^2.$$

The pressure distribution in the cross-section of the outlet nozzle is obtained by integration of the momentum balance equation along the radius with the boundary condition  $p(r_m) = p_{out}$ . It leads to the following expressions for  $p$  and  $w$ :

$$p = \frac{\rho}{2}(u_m^2 - u^2) + p_{out}, \quad w = \sqrt{\frac{2}{\rho}(p_{in} - p_{out}) - u_m^2 - \frac{2}{\rho}\Delta p_2 + w_\Sigma^2} \quad (5)$$

On the other hand, one can write:

$$m_\Sigma = \rho\varphi\pi r_{out}^2 w, \quad u_m = \frac{m_\Sigma R_2 B}{\rho F_2 r_m}, \quad r_m = r_{out}\sqrt{1-\varphi}, \quad w_\Sigma = \frac{m_\Sigma}{\rho F_p},$$

$$\Delta p = \xi_2 \frac{1}{2\rho} \left(\frac{m_\Sigma}{F_2}\right)^2 \left(1 - \frac{m_1}{m_\Sigma}\right)^2.$$

Substituting the values of  $w, u_m, \Delta p_2$  and  $w_\Sigma$  into expression for  $w$  in (5), we find:

$$m_\Sigma = \frac{F_{out}\sqrt{2\rho(p_{in} - p_{out})}}{\sqrt{\frac{1}{\varphi^2} + \frac{A}{1-\varphi^2} + \Delta}}, \quad (6)$$

$$A = \frac{\pi R_2 r_{out} B}{F_2}, \quad \Delta = \xi_2 \left(\frac{F_{out}}{F_2}\right)^2 \left(1 - \frac{m_1}{m_\Sigma}\right)^2 - \left(\frac{F_{out}}{F_p}\right)^2. \quad (7)$$

Thus, the flow rate coefficient of the vortex chamber of the valve as final-control element is determined by the expression:

$$\mu = \frac{1}{\sqrt{\frac{1}{\varphi^2} + \frac{A^2}{1-\varphi} + \Delta}}. \quad (8)$$

If the valve contains a vortex chamber with  $R_1 = R_2 = R$  and  $F_1 = F_2 = F$ , the relation for  $A$  takes the form:

$$A_t = \frac{\pi R r_{out}}{F} \left(1 - 2\frac{m_1}{m_\Sigma}\right). \quad (9)$$

Let express the flow rates ratio  $\frac{m_1}{m_\Sigma}$  through the structural parameters of the supply pipelines from the branching-out point to the periphery of the vortex chamber in the valve. It is known that

$$\Delta p_1 = \xi_{thr} \frac{1}{2\rho} \left(\frac{m_1}{F_{thr}}\right)^2, \quad \Delta p_2 = \xi_2 \frac{1}{2\rho} \left(\frac{m_2}{F_2}\right)^2 \quad (10)$$

Since both supply pipelines enter the same swirl chamber within the valve, we have  $\Delta p_1 = \Delta p_2 = \Delta p^*$ , and, as a result:

$$\frac{m_1}{m_\Sigma} = \frac{1}{1 + \frac{F_2}{F_{thr}} \sqrt{\xi_{thr}/\xi_2}}. \quad (11)$$

From the formula (11) the area  $F_{thr}$  is determined which provides for the required flow rates ratio  $m_1/m_\Sigma$ .

The resistance of each of pipelines 1 and 2 is described by the relation:

$$\Delta P = \xi_2 \frac{1}{2\rho} \left(\frac{m_\Sigma}{F_2}\right)^2 \left(1 - \frac{m_1}{m_\Sigma}\right)^2. \quad (12)$$

For  $m_1 = 0$  from (12) it follows:  $\Delta P^* = \Delta P_{\max} = \xi_2 m_\Sigma^2 / (2\rho F_2^2)$ ; for  $m_1 = 0.5m_\Sigma - \Delta P^* = 0.25\Delta P_{\max}^*$ .

### 3 Experimental investigation of the vortex chamber characteristics with tangential ducts creating opposite flows

The investigations were carried out on a model device which enabled changing the diameters of the inlet ducts and the outlet nozzle. The separable outlet nozzles were made with a sharp entrance rim and a smooth rounded entrance. The device design enabled the height of the swirl chamber to be increased from 30 to 60 mm. The vortex chamber diameter is 90 mm, the flow swirl radius  $R_1=R_2=30$  mm.

One of the pipelines had a measuring washer installed on it for measuring flow rate  $m_2$ , on the other one a throttle was installed to regulate the 'flow rate distribution between the pipelines (Fig. 1). Downstream from the device the flow was directed to a tank through a stand throttle and measuring washer registering the total flow rate  $m_\Sigma$ . The pressure was measured during the tests at the entrance to the branching point –  $P_{in}$ , on the pipeline with washing  $\Delta P_p$ , on the vortex chamber  $\Delta P_{vc}$  and on the throttle  $1 - \Delta P_{thr}$ . The model device was run through at constant water flow rates  $m = 9, 12, 15$  and  $18$  kg/s and at the inlet pressure  $P_{in} = 14$  MPa. For each flow rate the dependence value was registered of the hydraulic resistance  $\Delta P_\Sigma = \Delta P_p + \Delta P_{vc}$  on the flow rates ratio  $\frac{m_1}{m_\Sigma}$ , the value of which varied from 0 to 0.5. The characteristics were read for each pair of inlet ducts with different sizes of the outlet nozzles. Also checked was the effect of the vortex chamber height on the flow rate characteristics. Each run-through was assigned an index consisting of three numbers, of which the first two indicated the diameters of the inlet ducts, while the third number gave the



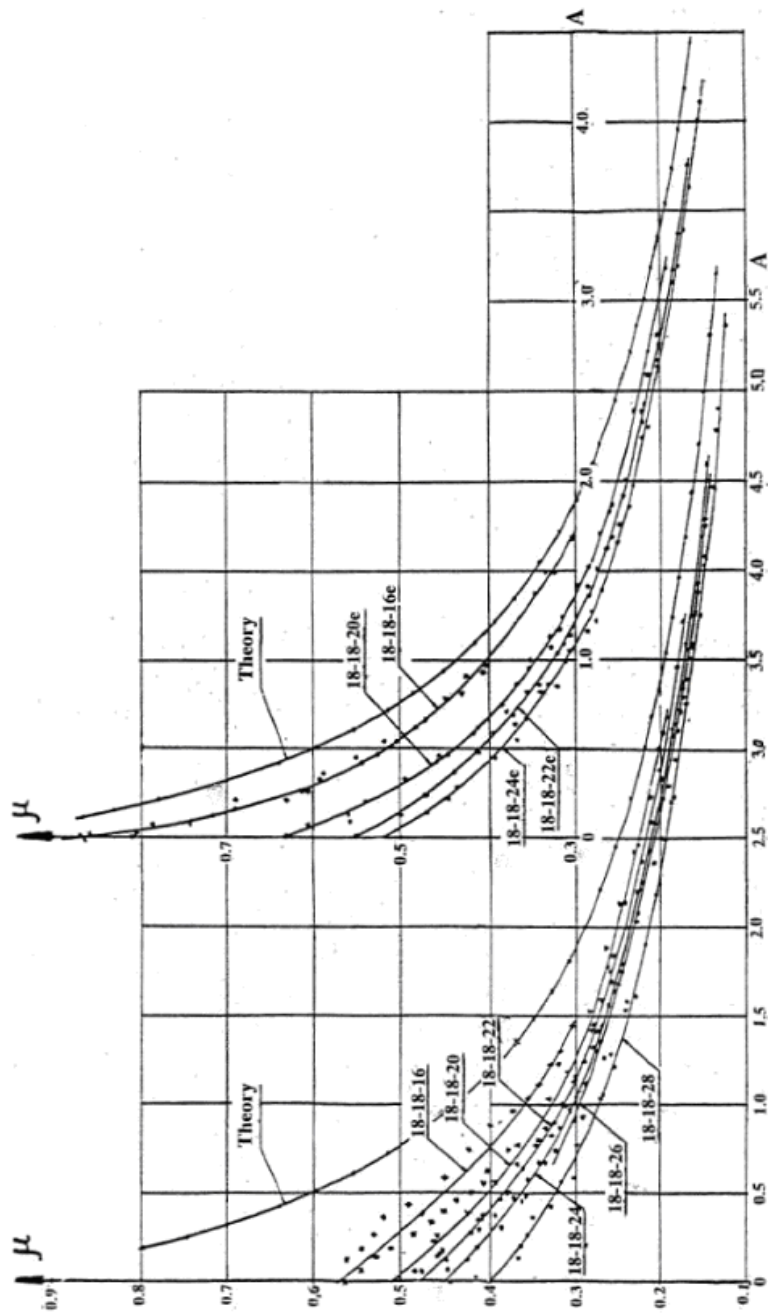


Figure 2: Effect from the entrance rim of the outlet nozzle.

diameter of the outlet nozzle. An additional index “e” was attached to the diameter of the nozzle with a smooth entrance.

The run-through results for different flow rates with outlet nozzles of each type are in good mutual correspondence as they are converted from one flow rate to another by the quadratic law (Fig. 2).

In the tests the minimal values of  $\mu$  were obtained equal to  $\mu_{min} = 0.14 \dots 0.12$ . A curve marked “Theory” is drawn in the figure which corresponds to the dependence  $\mu = f(A)$  for the ideal centrifugal nozzle [18]. Analysis of the dependence  $\mu = f(A)$  has shown that:

1. all the experimental dependences lie below the theoretical one, with those obtained for the nozzles with smooth entrances closer to the theoretical dependence, while it should be noted at the same time that comparison with the theoretical curve is rather conditional, because with the adopted outline for the vortex chamber operation there are losses connected with the flow rate redistribution between its ducts;
2. the character of the flow rate variation coefficient  $\mu = f(A)$  is similar to the theoretical picture;
3. for the same ducts and nozzle the flow rates calculated after the run-throughs with different flow rates cluster around a mean curve.

Tests of the device with the heights of the vortex chamber  $L = 30$  mm and  $L = 60$  mm showed that with increased height the value of the flow rate coefficient grew at the average of 7–10% (Fig. 3).

Comparison of experimental data on the variation of  $\Delta P_{\Sigma}$  and  $\Delta P_{thr}$  within the same range of flow rate ratio change has shown that at all the test regimes  $\Delta P_{thr}$  is significantly less than the device’s resistance and does not exceed 15–20% from  $\Delta P_{\Sigma}$ . Within this range of change in  $\frac{m_1}{m_{\Sigma}}$  the pressure drop on the distributing element increases relative to the initial value less than the total resistance.

Analysis of the obtained experimental data as well as of the adopted independent determining parameters has enabled a semi-empirical dependence to be found for the value of the flow rate coefficient of a valve with a vortex chamber that has tangential ducts to create opposing flows:

$$\mu = \mu_0 e^{-\left(\frac{kA}{L/d_{in}}\right)^{\frac{2}{3}}} \quad (13)$$

where  $k$  is a dimensionless coefficient taking account of the parameter that characterizes the ratio of the rounding-off radius of the entrance rim of the

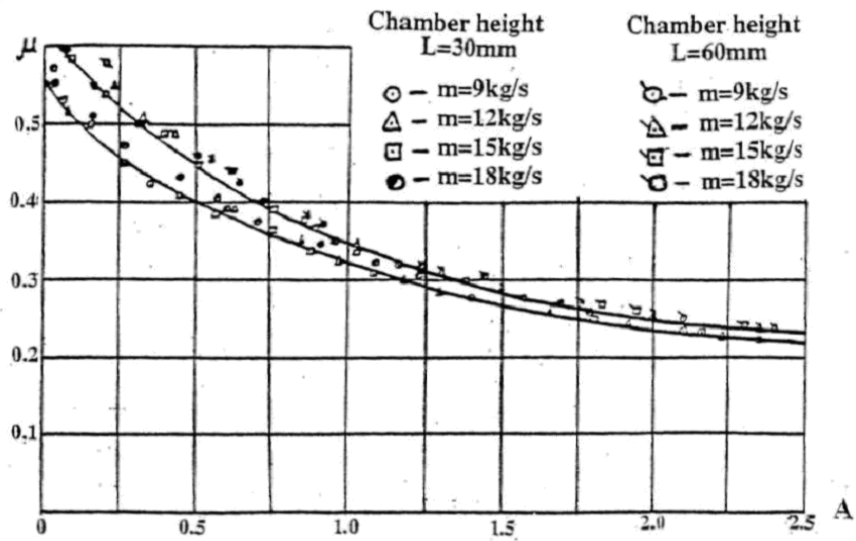


Figure 3: Test results for the model device with different heights of the vortex chamber.

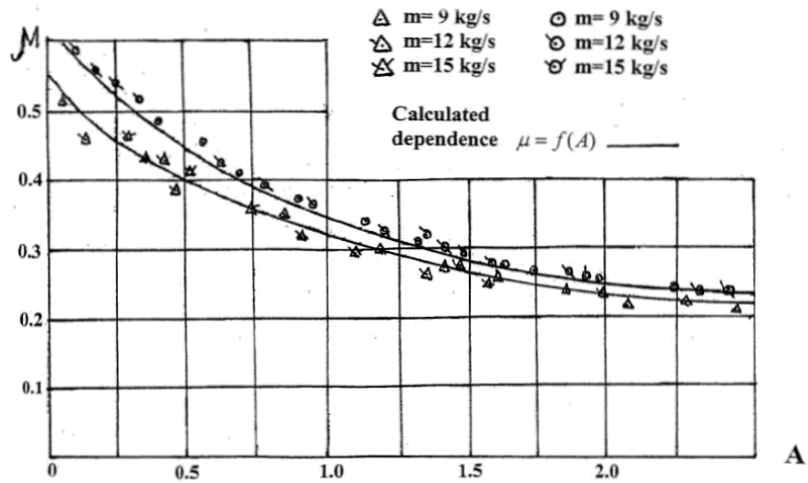


Figure 4: Test results for the model device in different assemblage versions at different flow rates.

outlet nozzle to the radius of the latter. Fig. 4 presents the values of the device's flow rate coefficient, experimental and calculated using dependence (13).

#### 4 Design and characteristics of the experimental valve

Figure 5 presents the structure of the experimental swirl valve developed at the IIM and operating in the mode considered above [14]. The valve comprises body 1 with swirl chamber 2, inside which tangential ducts 3 and 4 create opposing flows. The body contains sleeve 10 with transfer ports 9 for the passage of the working medium from the inlet chamber to tangential duct 4. Coaxially with duct 3 regulating element 5 is installed in the body, consisting of cylindrical jacket 8 and central rod 7 with contoured head 6 interconnected by ribs 11. The rod of the regulating element is connected with drive shaft 12.

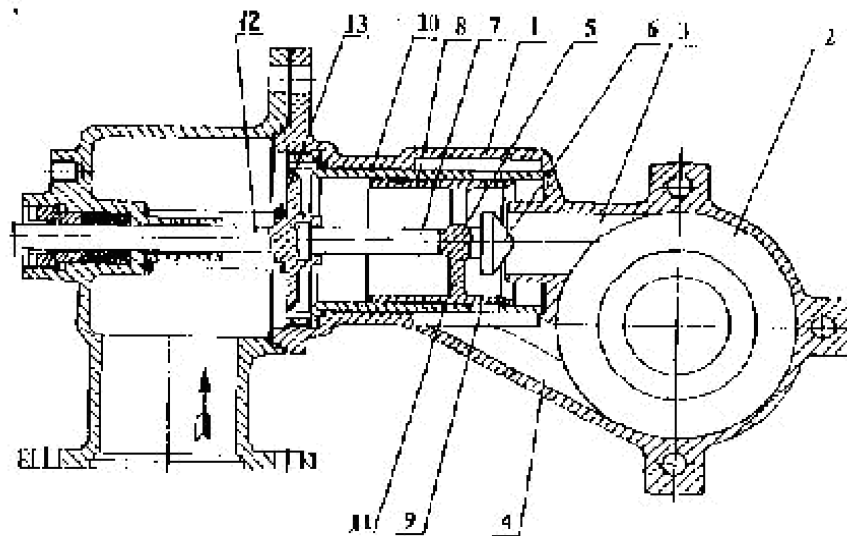


Figure 5: Structure of the experimental valve with a swirl chamber for opposing flows.

As the regulating element is moved by drive shaft 12, transfer ports 9

begin to be covered, which terminates the equality of the flows through ducts 3 and 4 and creates a rotating flow in the swirl chamber, thereby raising the hydraulic resistance of the valve. After all the transfer ports have been covered the further movement of the regulating element brings its contoured head into interaction with the entry to duct 3, further increasing the resistance of the valve. The required flow rate characteristic of the valve is provided for by contouring the transfer ports in sleeve 10 and the head of rod 7. In order to ensure the leak-tightness of the valve when fully closed, drive shaft 12 is fitted with screen 13, for which the sleeve bevel serves as the seat.

The cavitation characteristics of the valve are shown in Fig. 6. They were obtained under the constant inlet pressure  $p = 1.4$  MPa at positions of the regulating element expressed in percent of the total length of its travel.

As can be seen from the obtained data, the swirl valve, while providing for a wide range of flow rate regulation, features improved cavitation characteristics. At the position of the regulating element relative to duct 3 that corresponds to 25% of its total travel the moment of cavitation onset (i.e. start of the deviation of the flow rate characteristic from linear dependence) corresponds to the ratio  $p_{out}/p_{in} \approx 0.18$ . The value of this pressure ratio shifts towards the lower value region with the growing intensity of the flow swirl in the swirl chamber (and rising hydraulic resistance of the valve).

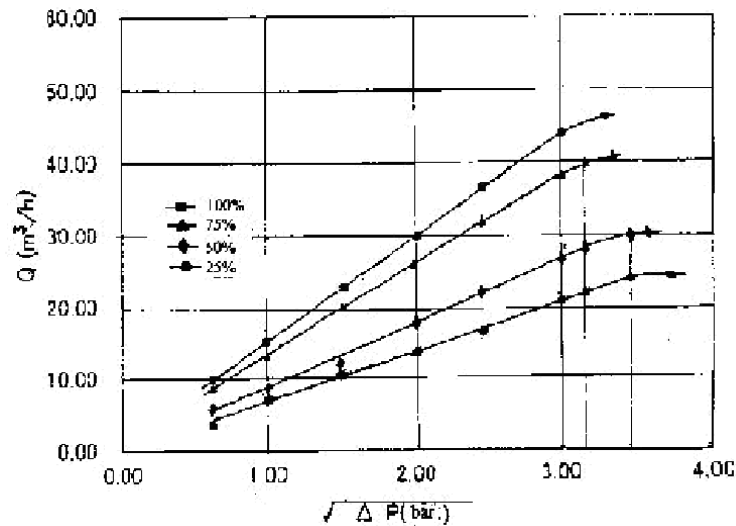


Figure 6: Cavitation characteristics of the experimental valve.

## 5 Conclusion

1. The equations have been derived for calculating the value of the vortex valve flow rate depending on the geometrical parameters of the vortex chamber as well as the value of the ratio between the flow rates through its tangential ducts.
2. As a result of the experimental investigation of a model device the dependences have been obtained of the flow rate coefficient value on the ratio between the flow rates through the tangential ducts for different variants of the vortex chamber design parameters; the influence on these data has been discovered of the value of the rounding-off radius of the entrance rim of the chamber outlet nozzle, of the chamber height.
3. Based on the analysis of the adopted independent dimensionless parameters and of the obtained experimental data, a semi-empirical dependence is proposed to determine the value of the flow rate coefficient of the valve for the given geometrical parameters of the vortex chamber as well as the ratio between the flow rates through the tangential ducts.
4. A valve design with a swirl chamber based on opposing flows is described, including its cavitation characteristics. It has been obtained that as flow throttling increases, cavitation onset shifts towards the region of smaller values of the  $p_{out}/p_{in}$  ratio.

## Nomenclature

$d_{out}$	diameter of the vortex chamber outlet nozzle;
$m_1$ and $m_2$	mass flow through lines 1 and 2 respectively;
$m_{\Sigma}$	total mass flow through the chamber;
$F_1$ and $F_2$	areas of inlets from lines 1 and 2 respectively;
$F_p$	cross-section of the tube supplying element of the valve;
$F_{out}$	area of the outlet nozzle;
$F_{thr}$	passage cross-section of the distributive element of the valve;
$L$	height of the vortex chamber;
$p$	pressure in the flow;
$p_{in}$	entry pressure before separation between lines 1 and 2;
$p_{out}$	pressure at the valve exit;
$\Delta p_2$	pressure loss to chamber periphery in line 2, equal to similar loss in 1;

$r$	distance from the nozzle axis to liquid particle in the nozzle;
$r_{out}$	radius of the vortex chamber outlet nozzle;
$R_1, R_2$	swirl radii of the flows entering the vortex chamber through lines 1 and 2;
$u$	tangential component of the velocity in the outlet nozzle;
$V_{in1}, V_{in2}$	flow velocities at the chamber entrance from lines 1 and 2 respectively;
$V_{in}$	resulting velocity of the flow in the chamber at radius $R$ ;
$w$	axial component of the velocity in the nozzle;
$w_{\Sigma}$	velocity in the pipeline (before separation between lines 1 and 2 );
$\mu$	flow rate coefficient of the outlet nozzle;
$\varphi$	filling coefficient of the nozzle;
$\rho$	density of the working body;
$\xi_{thr}$	loss coefficient in line 1 relative to velocity $v_{thr}$ in the passage cross-section of the distributive element of the valve;
$\xi_2$	pressure loss coefficient in line 2 relative to the mean velocity in area $F_2$ ;

## References

- [1] C. Samuel Martin, H. Medlarz, D.C. Wiggert, and C. Brennen, *J. of Fluids Engineering* **103**, 567 (1981).
- [2] N. Berchiche, M. Grekula, and G. Bark, Proc. of CAV'03, Osaka, Japan (2003).
- [3] Y. Lecoffre, J. Marcoz, and B.Valibouse, *Cavitation Erosion in Fluid Systems*, ASME, p. 133 (1981).
- [4] Y. Lecoffre, A. Archer, In: *Third International Symposium on Cavitation*, Grenoble, France (1998).
- [5] W.J. Rahmeyer, H.L. Miller, and S.V. Sherikar, *J. ASME* **210**, 64 (1995).
- [6] S.A. Taylor, Patent GB 2 259 585 A, Cl. F15c 1/16 (1991).
- [7] A. Mayer, Patent US 3674044, Cl. F15c 1/16 (1970).
- [8] G.F. Stilles, *Instrum. Technol.* **14**, 46 (1967).

- [9] R. Knapp, J. Daily, and F. Hammit, McGraw-Hill Book Co., N.Y. (1970).
- [10] D.N. Wormley and H.H. Richardson, Trans. ASME, ser. D **92**, 369 (1970).
- [11] R.F. Reydon and W.H. Gauvin, Canad. J. Chem. Eng. **59**, 14 (1981).
- [12] M.P. Levitsky, In: *International Symposium on Multi-Phase Flow and Transport Phenomena*, Antalya, Turkey, p.608 (2000).
- [13] Yu. F. Dityakin, L.A. Klyatchko et al., *Liquid dispersion* (Mashinostroyeniye, Moscow, 1977).
- [14] M.P. Levitsky, Patent WO 02/50456, Cl. F16K (2000).